OBJECT SPACE RECONSTRUCTION

[FOR [ERS-1] [STEREO] SAR] [AND] [FOR PERSPECTIV IMAGES]

V. Sasse

Institute for Photogrammetry and Engineering Surveys

University of Hannover, Germany

ISPRS Commission II

During the last years a new type of „object space algorithm“ for surface reconstruction has been applied to optical sources mainly. Nevertheless, the adjustment based algorithm is not sensor specific from theory. Especially sensors representing nature in strongly distorted images, seem to be predestinated for the object space reconstruction. Some algorithmic improvements were suggested.

Key Words: adjustment with numerical differentiation, bicubic splines, orthoimage, digital elevation model, correlation, feature based matching, multi sensoral, SAR, photo resp. perspective

1. INTRODUCTION

Firstly, it is an interesting task, to use advanced SAR imaging models together with object space algorithms. Secondly, the rectification of SAR images(p.e.ERS-1) is strongly dependent on the availability of digital elevation models. Using stereo SAR or even multi SAR together with pyramid technics within this algorithmic context a major disadvantage of SAR will be eliminated

Opposite to common correlation technics, several images of different sensors(SAR, perspective, ...) can be processed in one step. In theory there is no limit for the number of images involved. Therefore it is intended to increase the accuracy of results by increase of observations.

A major advantage of this sophisticated and therefore time consuming approach is that it implies the model into the matching process. There is no other algorithm which can reduce the disturbance by geometric distortion more than this one.

2. BASIC ALGORITHM

It is basically possible to integrate any type of transformation function. FIGURE 1. explains the geometric relationship between object and image space for radar and for perspective images. The number of images shall not imply that there is a limitation to stereo for any

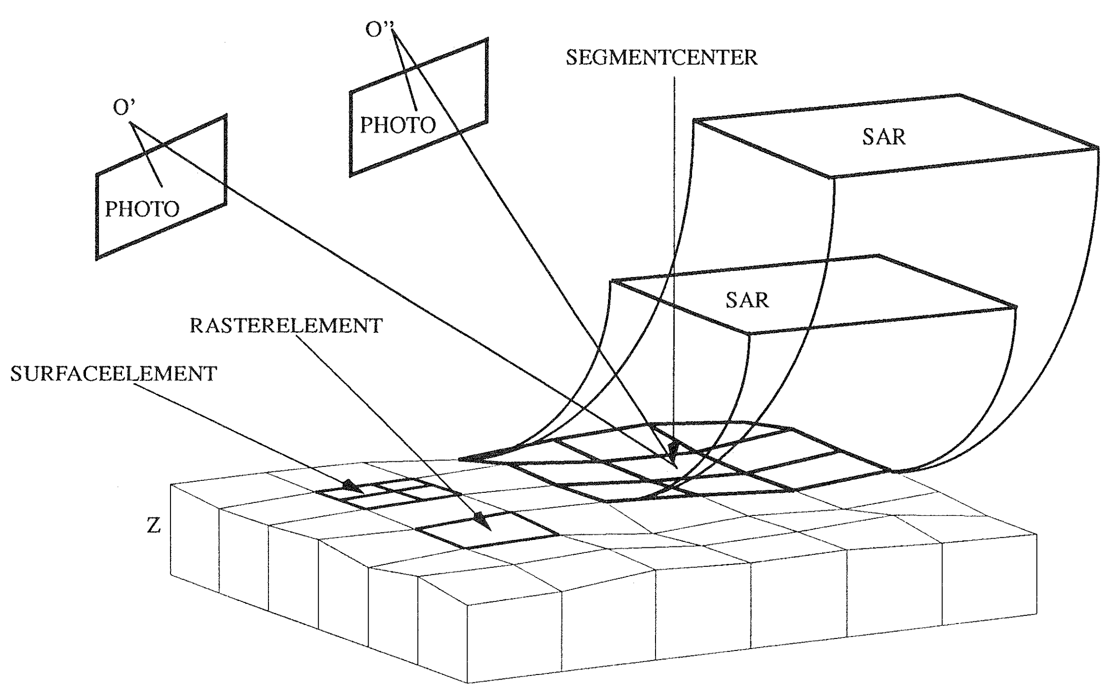

FIGURE 1. Geometric relationship between object and image space for radar and for perspective images

type of sensor.

Imagine, you have a given approximated raster of heights of some resolution. So far your surface is divided into rasterelements. Each rasterelement consists of another raster of $s_1 \cdot s_2$ surfaceelements. Meaning, surfaceelements are less coarse than rasterelements.

By means of a bilinear interpolation for every surfaceelement an estimation of height can be done. All surfaceelements are dependent on the corner heights of one rasterelement. Up to this step, there are 4 unknowns for one rasterelement, where there are $s_1 \cdot s_2$ observations.

Each image takes part of the observation of surface. Using the geometric transformation function from object space into image space, each image delivers one intensity for each surfaceelement. The first assumption for an adjustment will be:

„If the image model is correctly defined, you can derive the correct surface heights for all rasterelement corners minimizing the sum of squares of intensity differences for the collected number of surfaceelements."

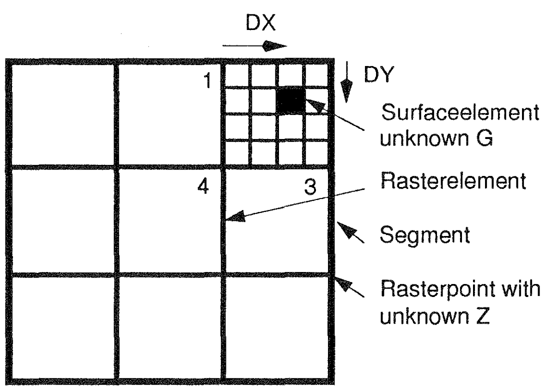

FIGURE 2. Dependencies of grids, element definitions

$$Z(x,y) = (1-dx)(1-dy)Z1 + dx(1-dy)Z2 + dy(1-dx)Z4 + dxdyZ3 \qquad \text{(EQ 1)}$$

See FIGURE 2. and (EQ 1) where the $Zi, i = 1,...,4$ are the heights of the surrounding rasterelement corners and dx and dy are the distances from the upper left corner.

$$vs(Z) = \sum dGs(i,Z) \qquad \text{(EQ 2)}$$

In (EQ 2) $vs(Z)$ are the residuals of surfaceelements at height Z and the $dGs(i,Z), i = 2,...,n\ (n \leftarrow \text{number'of'images})$ are the evaluated intensity differences between each image compared with image 1.

Under ideal circumstances, it is feasible to evaluate the same basic albedo for any surfaceelement from any image. As a matter of fact some kind of radiometric corrective parameters are evidently necessary. By means of the radiometry parameters all images are to be corrected relatively, adopting one image as a kind of basis. Depending on the number of images and the number of transformation coefficients we have to cope with additional unknowns within the model. The second assumption for an adjustment will be:

„You can derive the correct radiometric relationship between all images defined by polynomial functions of some degree minimizing the sum of squares of intensity differences for the collected number of surfaceelements."

$$vs(R) = \sum dGs(i,R) \qquad \text{(EQ 3)}$$

Similar to (EQ 2) the (EQ 3) informs about the residual evaluation, this time in respect to radiometric unknowns R

3. ALGORITHM SPECIALS

3.1 Numerical differentiation

The adjustment uses „numerical differentiation" enabling the system to cope with any kind of ugly geometric transformation function. Therefore, to extend the abilities the only requirement for the programmer will be, to apply a new transformation formula. Even iterative formulas are possible, because no analytic differentiation is needed. The requirement of the usage of numerical differentiation is caused by the iterative SAR-formula.

3.2 Two step method

For stabilising purposes the adjustment is done with a two step method. During the first step, only the geometrical unknowns(Z) are derived, while the radiometric unknowns keep their approximation values. Of course this approximation should not be too coarse respectively not a common value for any kind of image. We explain that below. Within the second step all unknowns are members of the iterative adjustment. During each iteration the number of function calls is at least the number of unknowns. And for every surfaceelement the intensity has to be evaluated from every image.

3.3 Bicubic spline interpolation

Image intensities are stored as raster data, normally. Because the data availability of discrete points in a fixed sized raster results in the necessity of interpolation, the data representation cannot be called continuous. On the other hand the numerical differentiation is intended for functions which are continuous and which have continuous first and second derivatives (although it will usually work if the derivatives have occasional discontinuities). Therefore the normal data representation is of no good use.

We solve the problem with a bicubic spline interpolating surface. The conversion determines a bicubic spline interpolant to the set of image raster points $(x_q, y_r, f_{q,r})$, for $q = 1,2,...,m_x; r = 1,2,...,m_y$. The spline is given in the B-spline representation

$$s(x,y) = \sum_{i=1}^{m_x} \sum_{j=1}^{m_y} c_{ij} M_i(x) N_j(y) \qquad \text{(EQ 4)}$$

such that

$$s(x_q, y_r) = f_{q,r} \qquad \text{(EQ 5)}$$

where $M_i(x)$ and $N_j(y)$ denote normalised cubic B-splines, the former defined on the knots λ_i to λ_{i+1} and the latter on the knots μ_j to μ_{j+4}, and the c_{ij} are the spline coefficients.

Now the object space algorithm will use the coefficients to calculate the image intensity values of a bicubic spline from its B-spline representation. This stabilises the adjustment process as it is a mathematical approach with less disturbing approximations, no discontinuities.

The following FIGURE 3. is an illustration using just the one dimensional case. The footings or in other content the knots of the spline are understood as the image raster positions. Thus we do not have to put up with loss of information. On the contrary, we introduce information into each position, because these B-splines take the surrounding pixels into account.

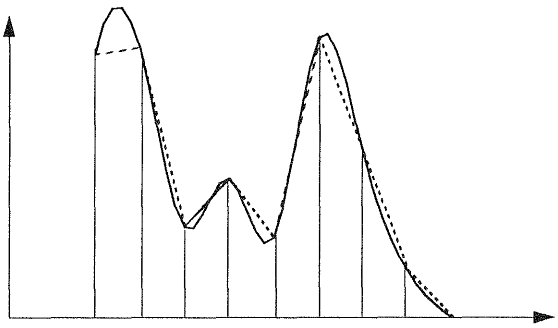

FIGURE 3. B-spline interpolation of intensity row

3.4 „Segmentation"

Obviously, the described system tends to need a lot of computer memory. Actually one would like to evaluate the unknowns of the area of interest within one single step, in other words within one single adjustment. But as the costs of this sophistication are too high the limitation into segments of the entire area is advised (see FIGURE 1. and FIGURE 2.). Step by step every segment is worked out, while the former results of one segment assists the approximation of unknowns for the next segment and so on. Besides, this segment approach has also some algorithmic advantages, as follows.

3.5 Feature based

Within each segment one has to take care of sufficient structural image information. Like within image correlation it is adequate to work feature based avoiding any defective task within areas of homogeneous intensities where image noise has the major misleading effects. A pattern recognition methodology has been applied to the system.

The applied interest operator investigates the error ellipses within the moving matrices of interest size. At first all gradients within the matrice are computed. Use either the sobel or the roberts gradient g_x and g_y. On this basis the covariance matrice is:

$$N = \begin{bmatrix} \sum g_x^2 & \sum g_x g_y \\ \sum g_x g_y & \sum g_y^2 \end{bmatrix} \qquad \text{(EQ 6)}$$

The next derivations are eigenvalues λ and determinants det given by the formulas in (EQ 7) and (EQ 8):

$$\lambda = \frac{\sqrt{\sum g_x^2 + \sum g_y^2 \pm \left(\left(\sum g_x^2 - \sum g_y^2\right)^2 + 4\left(\sum g_x g_y\right)^2\right)}}{2} \qquad \text{(EQ 7)}$$

$$det\left|\begin{bmatrix} \sum g_x^2 - \lambda & \sum g_x g_y \\ \sum g_x g_y & \sum g_y^2 - \lambda \end{bmatrix}\right| = 0 \qquad \text{(EQ 8)}$$

The relationship q between the two eigenvalues λ is a measure of the elliptical outlook:

$$q = 1 - \frac{\lambda_1 - \lambda_2}{\lambda_1 + \lambda_2} \qquad \text{(EQ 9)}$$

Secondly, structures will have a high weight w in respect to the surroundings. Thus we use the point error σ_p and the trace sp_Q as defined:

$$\sigma_p^2 = \sum g_x^2 + \sum g_y^2 = sp_Q \qquad \text{(EQ 10)}$$

with $Q = N^{-1}$ for the last step:

$$w = \frac{1}{sp_Q} = \frac{detN}{spN} \qquad \text{(EQ 11)}$$

This algorithm is applicable to any image type. In the actual case we need the orthoradar respectively the orthophoto for our feature control. This approximated unknown heights are good enough for these purposes. After the registration into orthoimages using the transformation functions below it is now possible to create context images with the above formulas. They deliver the texture values (see (EQ 11)) which are transformed into image intensities. The object space algorithm is now context oriented or in other words feature based.

3.6 Pyramids

Last not least in this chapter it is a matter of interest within every adjustment to get good approximations. Concerning the height Z an acceptable way is given by so called pyramid technics. If there is no digital elevation model available, we start within the top of the pyramid and work down. It is one way to use the same algorithm on each level, concerning SAR this is advisable. On the other hand feature based matching within image space can speed up the computation evidently. And for perspective images we prefer that method.

3.7 Phase correlation

The approximation evaluation for radiometric unknowns uses again the orthoimages within the phasecorrelation algorithm. To define the translation between two images to be compared they have to be transformed into frequency domain. The cross spectrum is the complex product of the spectres of the images. This can be separated into amplitude $|S^* \cdot S|$ (with S^* as the conjugate of S) and phase. The following equations give a short introduction into it:

$$P^{-1}{}_{(x,y)} = f(e^{i\varphi}_{(u,v)}) \qquad \text{(EQ 12)}$$

with the cross spectrum $e^{i\varphi}$ and (u, v) as discrete frequencies in x and y direction. Derive P by inverse two dimensional fourier transformation. The maximum determines the position of least phase differences.

An extension of the algorithm in comparison with others consists of the possibility to inject a certain definable amount of amplitude information. This is done by multiplication of the cross spectrum with a weight function:

$$H_{(u,v)} = \frac{1}{\left|S_{1,(u,v)} \cdot S_{2,(u,v)}\right|^{\alpha}} \qquad \text{(EQ 13)}$$

with $0 \le \alpha \le 1$

By means of the weight function there exists a connection between productmoment and phase correlation. The injection of 100% amplitude information equals them. But for the correlation of images with high radiometric differences a reduction of amplitude information increases the probability of corrected matches. In FIGURE 4. the overlap area of two images is pointed out.

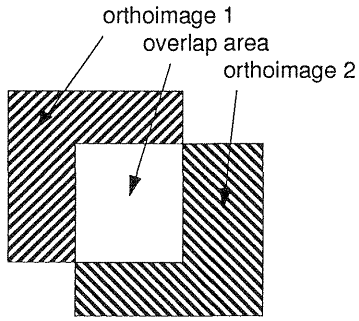

FIGURE 4. overlap of orthoimages from matching

3.8 Lookup polynomials

From the overlap area we can evaluate a simple lookup table and in a second step any polynomial with any FIGURE 5. degree. Actually, it is a matter of visualize and decide. An operator input should be the best way for a correct decision during the adjustment process. See FIGURE 5. for an estimation of the radiometric unknowns

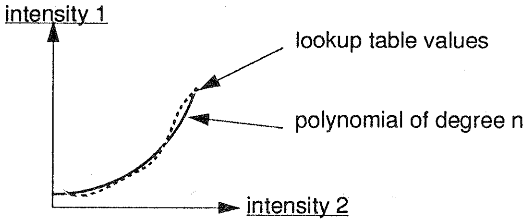

FIGURE 5. estimation of the radiometric unknowns

4. Transformation functions

4.1 SAR

Talking about SAR we mean the „slant range presentation". Sometimes, this is also denoted as a slant plane geometry. As a matter of fact ground range images are not considered within this work. The following FIGURE 6. gives a short overview from the relationship between surface, slant range and ground range.

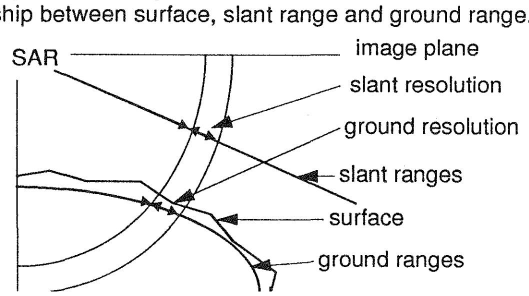

FIGURE 6. slant range presentation and others

The doppler equation F_x and the range equation F_y are as follows:

$$F_x: \frac{\lambda f_{DC}}{2} - \frac{(\dot{p}-\dot{s})\,(p-s)}{|p-s|} = 0 \qquad \text{(EQ 14)}$$

$$F_y: r - |p-s| = 0 \qquad \text{(EQ 15)}$$

where the parameters are explained in the following table 1: as well as partially in FIGURE 1. on the first page:

table 1: parameters of range and doppler equation

ground point	$p = (x, y, z)^T$
sensor position	$s = (x_s, y_s, z_s)^T$
ground point velocity vector	$\dot{p} = (\dot{x}, \dot{y}, \dot{z})^T$
sensor velocity vector	$\dot{s} = (\dot{x}_s, \dot{y}_s, \dot{z}_s)^T$
radar wave length	λ
doppler frequency	f_{DC}
range and time(phys.coord.)	r, t
offsets in range and time	r_0, t_0
pixel spacing/scaling in r, t	m_r, m_t
image coordinates	x, y

4.2 PHOTO

The perspective transformation is explained by the following collinearity equations (EQ 16) and (EQ 17):

$$x = x_0 - c\frac{i\,(p-s)}{k\,(p-s)} \qquad \text{(EQ 16)}$$

$$y = y_0 - c\frac{j\,(p-s)}{k\,(p-s)} \qquad \text{(EQ 17)}$$

table 2: parameters of collinearity equations

ground point	$p = (x, y, z)^T$
sensor position	$s = (x_s, y_s, z_s)^T$
rotation tensor	(i, j, k)
focal length	c
image coordinates	x, y
focal point	x_0, y_0

5. Preprocessing

Preprocessing could be understood as the task of the production of slant range images from received frequencies or scanning analog images or noise reduction adaptive filtering of images. Of course this has to be done sometime. Here we want to outline the estimation of the outer orientation.

As already mentioned, the adjustment approach is fairly open for any changes when considering to extend the number of unknowns. Of course, the improvement of the outer orientation during the adjustment will be the next future investigation. But anyhow, a good estimation of the orientation is necessary.

5.1 SAR

The following FIGURE 7. explains the steps.

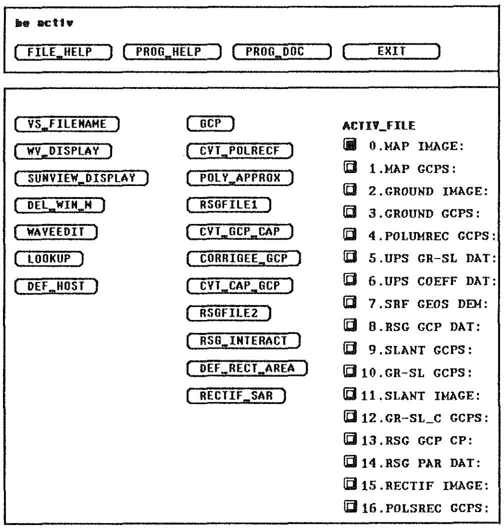

FIGURE 7. SAR orientation

Besides, this is the outlook of the system module on a SUN workstation. The basic language for the system PV_WAVE (VDA) controls all actions including remote procedure calls(RPC) onto either other SUN workstations or the vector computer of the regional computer centre. External programs are written in C or FORTRAN.

The explanation concentrates on some buttons inside the centre column. GCP's (ground control points) have to be measured connecting the image and the object coordinate systems. With the help of this split screen tool and digitized maps everything to be done is fully digital.

Preferably prerectified images (using polynomial rectification) assist the correct control point measurement. After backtransformation into the slant range presentation CORRIGEE_GCP supports corrections with lot of image processing tools.

With RSG_INTERACT the interactive and iterative data handling for the actual orientation definition follows. Parts of this module base on algorithms and programs of the DIBAG(see RAGGAM). The four major input values are:

table 3: SAR model parameter

range offset
range scale
flying height
incidence angle

Afterwards DEF_RECT_AREA serves as object space area definition module for the DEM based orthoradar production (DEM = digital elevation model) with the finishing RECTIF_SAR. At this stage the DEM must be available from any source transformed into the projection of the digitized map.

5.2 PHOTO

Now pay attention to FIGURE 8.

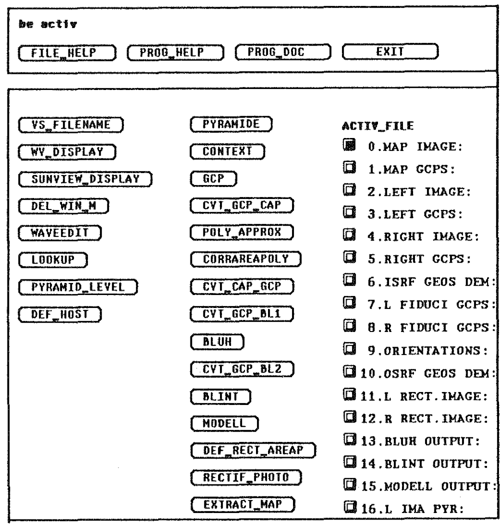

FIGURE 8. PHOTO orientation

Starting with PYRAMIDE the number of levels defines the number of loops through the whole orientation and DEM approximation. From CONTEXT we will get the image base for the feature based approach. GCP doesn't differ from above.

CORRAREAPOLY computes the feature based matching within image space. It uses the product moment coefficient. The precise description stands out of the topic of this paper.

The bundle block adjustment of the university of Hannover (BLUH) is itself another system introduced here. The lot of correlation points, one example consisted of 36000 points, together with the GCP's gives a stable platform for a high precision orientation definition. The included data snooping aids to get rid of erroneous correlation results.

Using BLINT and MODELL the temporary result of a refined equally spaced DEM can be derived. The end builds RECTIF_PHOTO with again the temporary result of an orthophoto.

6. RESULTS AND CONCLUSIONS

The current status is not from a time of final results. However, some empirical results of other authors who used similar approaches for photos were confirmed.

For simulated images a lot of tests manifested, that the adjustment enables the definition of heights with highest accuracy. The best measure for comparison we will get after transformation the accuracy from object into image space.

The image space results were better than two percent of a pixel. This is neither the a variance nor a standard deviation, but the absolute error.

Based on these results we hope to continue to get good results when using ERS1 slant range images. The system should enable us to rectify SAR data even in areas where no acceptable DEM is available. A side effect is the simultaneous computation of such a DEM. Of course the application to real economic usage is beyond the actual scope.

The connection of this way of data analysis with a geocoded database is our concern in parallel and at the moment. From that a continuous investigation of land surfaces in respect to initial classification and change detection will be possible. The first step to enable the system to do that task is easy to realize just adding the data type respectively the transformation function MAP.

The object space reconstruction is born to be applied to radar processing. Any kind of image space matching has severe problems even when correlating simulated and real SAR data. If there exists a radar map of an area where new data have to be rectified, this approach should be applied.

7. LITERATURE

RAGGAM, H: An efficient object space algorithm for space borne SAR image geocoding, ISPRS, commission II, Kyoto

MEIER, E: Geometrische Korrektur von Bildern orbitgestuetzter SAR - Systeme, Doktorarbeit 1989, Zurich

LEBERL, F.W.: Radargrammetric image processing, artech house, 1990, Norwood

HAYES and HALLIDAY: The least square fitting of cubic spline surfaces to general datasets, J. Inst. Maths. Applics., 14, pp. 89-103, 1974

DE BOOR, C.: On calculating with B-splines, J.Approx. Theory, 6, pp. 50-62, 1972

EHLERS, M.: Untersuchungen von digitalen Korrelationsverfahren zur Entzerrung von Fernerkundungsaufnahmen, Doktorarbeit 1983, Hannover

HEIPKE, CHR.: Integration von Bildzuordnung, Punktbestimmung, Oberflaechenrekonstruktion und Orthoprojektion innerhalb der digitalen Photogrammetrie, Doktorarbeit 1990, Muenchen

FOERSTNER, W.: Prinzip und Leistungsfaehigkeit der Korrelation und Zuordnung digitaler Bilder, Vortrag Photogrammetrische Woche, 1985, Stuttgart